ISSN 1029-9599, Physical Mesomechanics, 2017, Vol. 20, No. 2, pp. 149–156. © Pleiades Publishing, Ltd., 2017.
Original Text © M.R.M. Aliha, F. Berto, A. Bahmani, P. Gallo, 2016, published in Fizicheskaya Mezomekhanika, 2016, Vol. 19, No. 6, pp. 5–12.

# Mixed Mode I/II Fracture Investigation of Perspex Based on the Averaged Strain Energy Density Criterion

**M. R. M. Aliha[1]*, F. Berto[2,3], A. Bahmani[1,4], and P. Gallo[5]**

[1] *Welding and Joining Research Center, School of Industrial Engineering, Iran University of Science and Technology, Narmak, Tehran, 16846-13114 Iran*
[2] *Department of Management and Engineering, University of Padova, Vicenza, 36100 Italy*
[3] *Department of Engineering Design and Materials, Norwegian University of Science and Technology, Trondheim, 7491 Norway*
[4] *Department of Mechanical and Mechatronics Engineering, University of Waterloo, Waterloo, ON N2L 3G1 Canada*
[5] *Department of Mechanical Engineering, Aalto University, Espoo, 02150 Finland*
* *e-mail: m_aliha@yahoo.com, mrm_aliha@iust.ac.ir*

Received June 20, 2016

**Abstract**—In this work, some recent mixed mode I/II fracture toughness results obtained from Perspex (or polymethylmethacrylate (PMMA)) with four simple cracked specimens subjected to the conventional three-point bend loading are reanalysed based on local energy concept. Although all the mentioned samples have been tested under the same and similar mode mixities, different fracture toughness envelopes were obtained for mixed mode I/II fracture of PMMA. The averaged strain energy density (SED) criterion has been applied in the past for different types of notched specimens (including U, V, O and keyhole notches). It is shown that the mixed mode tensile–in plane shear fracture toughness data obtained from the semicircular and triangular crack type specimens are successfully predicted for sharp cracked PMMA samples using the SED criterion.

**DOI:** 10.1134/S1029959917020059

*Keywords*: mixed mode I/II, PMMA, SED criterion, fracture toughness, semicircular and triangular specimens

## 1. INTRODUCTION

Cracks may initiate inside the structure of brittle engineering materials during their manufacturing process, assembling and production stage or even during their service life. Today, it is well established that the crack growth is one of the main reasons for the overall failure and brittle fracture in various engineering materials like brittle polymers, ceramics and rocks. Real cracked structures are often subjected to complex loading conditions. Therefore, the investigation of crack growth in brittle materials under any arbitrary combinations of tensile and shear (mixed mode I/II) loading is important for failure analysis in different engineering components and structures. Mixed mode brittle fracture is usually studied both experimentally and theoretically using suitable materials and test specimens. Perspex or polymethylmethacrylate (PMMA) has been recognized as a favourite material for evaluating the fracture characteristics of brittle materials. This is because of its certain advantages like: brittle fracture at room temperature, low cost, machinability and convenience of test sample preparation and optical transparency that allows direct observation of crack tip region and path of crack growth during the fracture processes. Moreover, as stated by Maccagno and Knott [1] a sharp crack can be introduced in the root of an artificially fabricated prenotch in PMMA by pressing a razor blade. Indeed, this simple method, eliminate time consuming and expensive process of fatigue precracking procedure which is applied for metals. Hence, it is reasonable to assume that the linear elastic stress field equations outlined by Irwin [2] or Williams [3] can provide good description for the stress/strain field near the tip of sharp precracks introduced in the laboratory scale PMMA test specimens. A review of literature indicates that several mixed mode I/II fracture experi-

ments have been conducted on PMMA using various test specimens. PMMA plates containing inclined centre cracks with respect to the far field uniform tension loading [4, 5], rectangular plates of PMMA having an inclined edge crack and subjected to a far field tensile load or a bending moment [6], the compact tension shear specimen [7], the diagonally loaded square plate containing an inclined centre crack [8], the centrally cracked Brazilian disc specimen subjected to diametral compression [9, 10], the semicircular and triangular bend specimen [11–14] and the asymmetric three or four-point bend loading specimens [1, 15, 16] are some of the test configurations used by the researchers for investigating the mixed mode I/II fracture behaviour of PMMA. There have also been some attempts for analysing and predicting the experimental results (such as critical fracture loads, stress intensity factors, fracture initiation direction and the trajectory of fracture growth) obtained from the aforementioned test configurations using theoretical based fracture models.

Different approaches such as stress, strain and energy methods have been proposed for investigating the brittle fracture phenomenon under mixed mode I/II condition. For example, maximum tangential stress [4], minimum strain energy density [17], maximum energy release rate [18], cohesive zone model [19] and mean stress [20] are some of the frequently used mixed mode I/II fracture criteria. These criteria provide theoretical framework for predicting the ratio of $K_{\mathrm{I}}/K_{\mathrm{II}}$ for any mode mixity (or combinations of modes I and II). In a recent paper, Aliha and coworkers [14] obtained a series of new fracture toughness data for PMMA by testing some edge cracked semicircular and triangular specimens subjected to three-point bend loading. They determined magnitudes of $K_{\mathrm{I}}$ and $K_{\mathrm{II}}$ for each specimen in the entire range of mode mixities from pure mode I to pure mode II and showed that different fracture envelopes are obtained depending on the shape and loading type of specimens.

A fracture model based on the strain energy density (SED) averaged over a control volume has been used successfully in the past by Lazzarin and Berto and coworkers [21–28] mainly for different types of notched samples containing U-, V-, O- and keyhole notches subjected to pure modes and also mixed mode I/III loading cases. In the present work, the application of SED criterion is examined for assessing the mixed mode I/II fracture results presented in Ref. [14] for different PMMA samples. Hence, in the upcoming sections of this paper, first the experimental activity performed by Aliha et al. [14] is briefly recalled and then the predictions of the averaged SED theory is presented for mixed mode I/II cracked PMMA specimens.

## 2. MIXED MODE I/II PMMA FRACTURE TOUGHNESS DATA

Recently, Aliha et al. [14] conducted mixed mode I/II fracture toughness experiments on PMMA using simple test specimens in the shape of half disc and triangle containing an edge crack and subjected to conventional three-point bend loading. Figure 1 shows the geometry and loading configuration of the mentioned specimens. For easy understanding, the specimens are designated as SCB (semicircular bend) and TB (triangular bend). Suffix "1" and "2" was used for inclined crack with symmetric supports and vertical crack with asymmetric loading supports, respectively.

The crack tip stress state can be changed in these specimens by changing either crack inclination angle $\alpha$ or the loading support distance $S_2$. Therefore, the stress intensity factors $K_{\mathrm{I}}$ and $K_{\mathrm{II}}$ are function of specimen geometry and its loading conditions (i.e. parameters such as applied load $P$, crack length $a$, disc radius $R$, base length of triangle $W$, thickness $t$, crack angle $\alpha$ and bottom loading roller distances from the crack $S$, $S_1$ and $S_2$). Thus, the mode I and mode II stress intensity factors of the mentioned specimens can be obtained by the following equations:

$$K_{\mathrm{I}} = \begin{cases} \dfrac{P\sqrt{\pi a}}{2Rt} Y_{\mathrm{I}}(a/R, S/R, \alpha) & \text{for SCB1,} \\ \dfrac{P\sqrt{\pi a}}{2Rt} Y_{\mathrm{I}}(a/R, S/R, S_1/R) & \text{for SCB2,} \\ \dfrac{P\sqrt{\pi a}}{2Wt} Y_{\mathrm{I}}(a/R, S/R, \alpha) & \text{for TB1,} \\ \dfrac{P\sqrt{\pi a}}{2Wt} Y_{\mathrm{I}}(a/R, S/R, S_1/R) & \text{for TB2,} \end{cases} \quad (1)$$

$$K_{\mathrm{II}} = \begin{cases} \dfrac{P\sqrt{\pi a}}{2Rt} Y_{\mathrm{II}}(a/R, S/R, \alpha) & \text{for SCB1,} \\ \dfrac{P\sqrt{\pi a}}{2Rt} Y_{\mathrm{II}}(a/R, S/R, S_2/R) & \text{for SCB2,} \\ \dfrac{P\sqrt{\pi a}}{2Wt} Y_{\mathrm{II}}(a/R, S/R, \alpha) & \text{for TB1,} \\ \dfrac{P\sqrt{\pi a}}{2Wt} Y_{\mathrm{II}}(a/R, S/R, S_2/R) & \text{for TB2,} \end{cases} \quad (2)$$

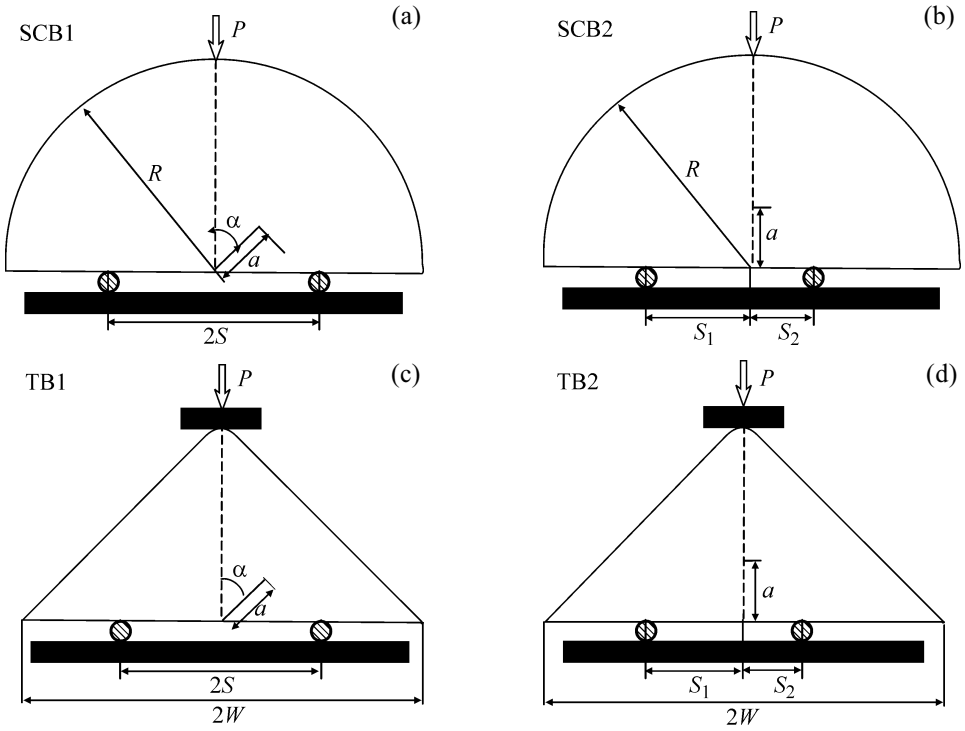


**Fig. 1.** Geometry and loading conditions of TB1, TB2, SCB1 and SCB2 specimens.

in which $Y_{\mathrm{I}}$ and $Y_{\mathrm{II}}$ are geometry factors that are functions of $a/R, a/W, S/R, S_1/R, S_2/R$ and α, SCB1, SCB2, TB1, TB2 are specimens. Six values $M^{\mathrm{e}}$ (0.0, 0.2, 0.4, 0.6, 0.8 and 1.0) were used in Ref. [14] to obtain the mixed mode fracture toughness values, where $M^{\mathrm{e}}$ is defined as:

$$M^{\mathrm{e}} = 2/\pi \arctan(K_{\mathrm{I}}/K_{\mathrm{II}}).$$

The overall dimensions of both SCB and TB specimen types were equal to the following values in the experiments of Ref. [14]: $R = W = 50$ mm, $S = S_1 = 20$ mm, $a = 15$ mm and $t = 5$ mm. Other parameters such as α and $S_2$ were considered as variable in [14]. Loading specifications and geometry factors of the tested specimens for different mode mixities have been presented in Table 1.

The corresponding values of mode I and mode II fracture toughness values for the considered mode mixities were obtained by recording the fracture load of the SCB1, SCB2, TB1 and TB2 specimens made of PMMA using Eqs. (1) and (2). A servohydraulic compression test machine (as shown in Fig. 2) was used for testing the specimens.

All the test samples were fractured from the tip of crack and, as it is obvious, from Fig. 3 the load–displacement curves obtained from the test samples demonstrated linear elastic fracture behavior, with negligible nonlinear deformation for PMMA at room temperature.

The obtained mixed mode I/II fracture toughness results have been presented in Fig. 4 in a $K_{\mathrm{I}}/K_{\mathrm{Ic}}$ –

**Table 1.** Loading specifications and corresponding geometry factors $Y_{\mathrm{I}}$ and $Y_{\mathrm{II}}$ for the investigated SCB and TB specimens

| Specimen | $M_{\mathrm{e}}$ | | | | | | | | | | | | | | | | | | | | | | | |
|---|---|---|---|---|---|---|---|---|---|---|---|---|---|---|---|---|---|---|---|---|---|---|---|---|
| | α | | | | | | $S_2$, mm | | | | | | $Y_{\mathrm{I}}$ | | | | | | $Y_{\mathrm{II}}$ | | | | | |
| | 1.0 | 0.8 | 0.6 | 0.4 | 0.2 | 0.0 | 1.0 | 0.8 | 0.6 | 0.4 | 0.2 | 0.0 | 1.0 | 0.8 | 0.6 | 0.4 | 0.2 | 0.0 | 1.0 | 0.8 | 0.6 | 0.4 | 0.2 | 0.0 |
| TB2 | – | – | – | – | – | – | 20 | 12.5 | 9.5 | 8 | 6.5 | 5 | 3.4 | 3.07 | 2.03 | 1.26 | 0.62 | 0 | 0 | 0.10 | 0.23 | 0.39 | 0.87 | 1.62 |
| TB1 | 0° | 10° | 26° | 38° | 45.5° | 52.5° | – | – | – | – | – | – | 3.4 | 3.24 | 2.79 | 2.11 | 1.35 | 0 | 0 | 0.48 | 0.88 | 1.11 | 1.13 | 0.86 |
| SCB2 | – | – | – | – | – | – | 20 | 14 | 11.5 | 9 | 7.5 | 6 | 1.8 | 1.64 | 1.44 | 1.22 | 0.68 | 0 | 0 | 0.09 | 0.20 | 0.34 | 0.76 | 1.41 |
| SCB1 | 0° | 12° | 23° | 31° | 37° | 42.5° | – | – | – | – | – | – | 1.8 | 1.66 | 1.27 | 0.73 | 0.16 | 0 | 0 | 0.40 | 0.70 | 0.84 | 0.98 | 0.85 |

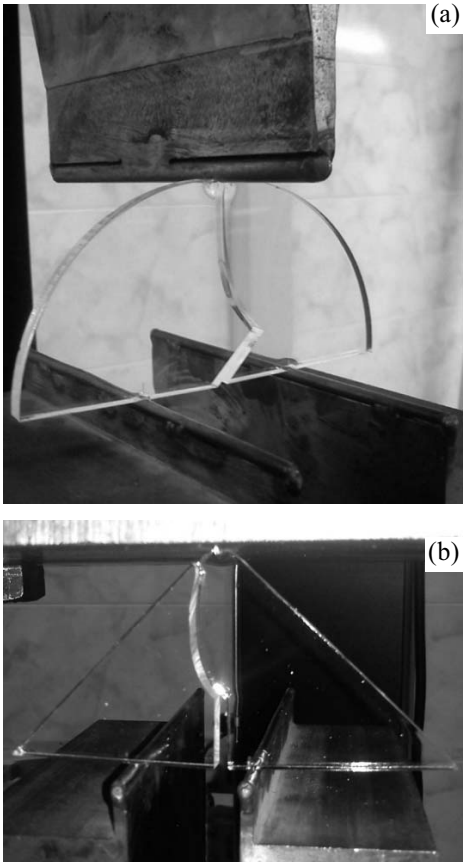


**Fig. 2.** Test setup for testing SCB (a) and TB (b) specimens made of PMMA.

$K_{II}/K_{Ic}$ diagram, in which $K_{Ic}$ is the pure mode I fracture toughness of PMMA. $K_I$ and $K_{II}$ are the critical values of stress intensity factors at the onset of fractures and corresponds to the fracture load of each tested specimen. The average $K_{Ic}$ obtained from the four specimens is 1.87 MPa $m^{0.5}$.

This value is in the range of 1–2 MPa $m^{0.5}$ reported in previous papers for fracture toughness of PMMA [8, 11–13, 29–31]. Figure 4 reveals that depending on the specimen shape and its loading condition, different fracture toughness results are obtained for a same material. These results are evaluated theoretically in the next section using the averaged SED criterion.

## 3. STRAIN ENERGY DENSITY AVERAGED OVER A CONTROL VOLUME: THE FRACTURE CRITERION

With the aim to assess the fracture load in notched PMMA components, an appropriate fracture criterion is required which has to be based on the mechanical behavior of material around the crack or the notch tip.

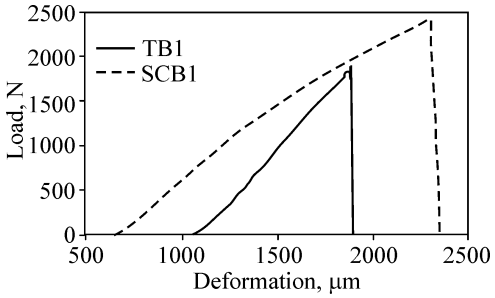


**Fig. 3.** Typical load–displacement curves obtained for the SCB and TB specimens.

In this section, a criterion proposed by Lazzarin and coauthors [21] based on the strain energy density (SED) is briefly described.

The averaged strain energy density criterion as presented in Refs. [21–28] states that brittle failure occurs when the mean value of the strain energy density over a given control volume is equal to a critical value $W_c$. This critical value is a material characteristic parameter and does not depend on the notch geometry and sharpness. Dealing with mode I loading, the control volume is considered to be dependent on the ultimate tensile strength $\sigma_t$ and the fracture toughness $K_{Ic}$ in the case of brittle or quasi-brittle materials subjected to static loading.

The method based on the averaged SED was formalized and applied first to sharp (zero radius) V-notches under mode I and mixed mode I/II loading [21] and later extended to blunt U- and V-notches [22–24]. When dealing with cracks, as in the present research, the control volume is a circle of radius $R_c$ centered at the crack tip (Fig. 5a). Under plane strain conditions, the radius $R_c$ can be evaluated according to the following expression:

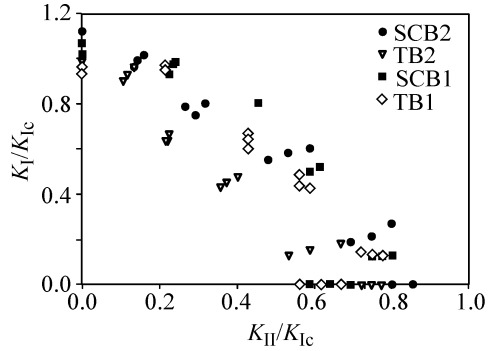


**Fig. 4.** Mixed mode I/II fracture toughness results obtained from SCB1, SCB2, TB1 and TB2 specimens.

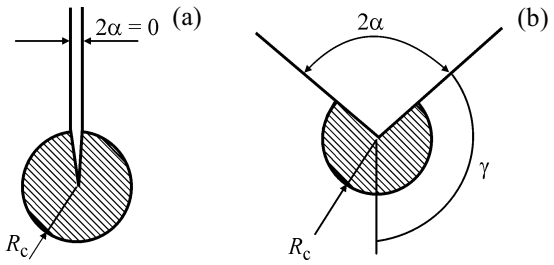


**Fig. 5.** Control volume for crack (a), sharp V-notch (b).

$$R_{1c} = \frac{(1+\nu)(5-8\nu)}{4\pi}\left(\frac{K_{Ic}}{\sigma_t}\right)^2, \quad (3)$$

where ν is the Poisson's ratio and $\sigma_t$ is the ultimate tensile stress of a flat specimen.

For a sharp V-notch, the critical volume becomes a circular sector of radius $R_c$ centred at the notch tip (Fig. 5b).

Dealing here with sharp notches under mode II loading, the control radius $R_{2c}$ can be estimated by means of the following equation first proposed in Ref. [27]:

$$R_{2c} = \frac{9-8\nu}{8\pi}\left(\frac{K_{IIc}}{\tau_t}\right)^2, \quad (4)$$

where $K_{IIc}$ is the mode II critical notch stress intensity factor and $\tau_t$ is the ultimate shear strength of the unnotched material and can be calculated approximately as

$$\tau_t = \sigma_t \Big/ \sqrt{2(1+\nu)}. \quad (5)$$

## 4. SED APPROACH IN FRACTURE ANALYSIS OF THE TESTED PMMA SPECIMENS

The fracture criterion described in the previous section is employed here to estimate the fracture loads obtained from the experiments conducted on the PMMA specimens.

As originally thought for pure modes of loading the averaged strain energy density criterion states that failure occurs when the mean value of the strain energy density over a control volume $\overline{W}$ reaches a critical value $W_c$, which depends on the material but not on the notch geometry.

**Table 2.** Experimental results. Overview of the data by using the proposed SED method for the SCB1 specimens

| α | $W_1$, MJ/m$^3$ | $W_2$, MJ/m$^3$ | $W_1/W_{1c} + W_2/W_{2c}$ | $(W_1/W_{1c} + W_2/W_{2c})^{0.5}$ |
|---|---|---|---|---|
| 0.0° | 0.712 | 0.000 | 0.858 | 1.016 |
| 0.0° | 0.793 | 0.000 | 0.956 | 1.073 |
| 0.0° | 0.879 | 0.000 | 1.059 | 1.129 |
| 12.0° | 0.665 | 0.087 | 0.904 | 1.044 |
| 12.0° | 0.744 | 0.099 | 1.015 | 1.106 |
| 12.0° | 0.736 | 0.095 | 1.000 | 1.097 |
| 23.0° | 0.501 | 0.355 | 1.026 | 1.112 |
| 23.0° | 0.494 | 0.355 | 1.018 | 1.107 |
| 23.0° | 0.501 | 0.355 | 1.026 | 1.112 |
| 31.0° | 0.190 | 0.594 | 0.936 | 1.062 |
| 31.0° | 0.211 | 0.649 | 1.027 | 1.113 |
| 31.0° | 0.194 | 0.594 | 0.941 | 1.065 |
| 37.0° | 0.013 | 1.105 | 1.331 | 1.266 |
| 37.0° | 0.012 | 1.033 | 1.243 | 1.224 |
| 37.0° | 0.013 | 0.963 | 1.161 | 1.183 |
| 42.2° | 0.000 | 0.707 | 0.842 | 1.007 |
| 42.2° | 0.000 | 0.594 | 0.707 | 0.923 |
| 42.2° | 0.000 | 0.830 | 0.988 | 1.091 |

**Table 3.** Experimental results. Overview of the data by using the proposed SED method for the TB1 specimens

| α | $W_1$, MJ/m$^3$ | $W_2$, MJ/m$^3$ | $W_1/W_{1c} + W_2/W_{2c}$ | $(W_1/W_{1c} + W_2/W_{2c})^{0.5}$ |
|---|---|---|---|---|
| 0.0° | 0.673 | 0.000 | 0.811 | 0.988 |
| 0.0° | 0.712 | 0.000 | 0.858 | 1.016 |
| 0.0° | 0.793 | 0.000 | 0.956 | 1.073 |
| 10.0° | 0.914 | 0.079 | 1.195 | 1.200 |
| 10.0° | 0.941 | 0.079 | 1.228 | 1.216 |
| 10.0° | 0.905 | 0.079 | 1.184 | 1.195 |
| 26.0° | 0.835 | 0.314 | 1.381 | 1.290 |
| 26.0° | 0.776 | 0.314 | 1.310 | 1.256 |
| 26.0° | 0.879 | 0.314 | 1.433 | 1.314 |
| 38.0° | 0.613 | 0.541 | 1.383 | 1.291 |
| 38.0° | 0.598 | 0.594 | 1.428 | 1.312 |
| 38.0° | 0.681 | 0.541 | 1.464 | 1.328 |
| 45.5° | 0.301 | 1.033 | 1.592 | 1.385 |
| 45.5° | 0.343 | 0.963 | 1.559 | 1.371 |
| 45.5° | 0.332 | 0.895 | 1.466 | 1.329 |
| 52.5° | 0.127 | 0.649 | 0.926 | 1.056 |
| 52.5° | 0.130 | 0.541 | 0.801 | 0.983 |
| 52.5° | 0.134 | 0.767 | 1.075 | 1.138 |

Under tension loads, this critical value can be determined from the ultimate tensile strength $\sigma_t$ according to Beltrami's expression for the uncracked material:

$$W_{1c} = \frac{\sigma_t^2}{2E}. \quad (6)$$

By using the values of $\sigma_t$ = 70 MPa and $E$ = 2950 MPa, the critical SED for the tested PMMA is determined as $W_{1c} = 0.83$ MJ/m$^3$ [31].

Under torsion loads, this critical value can be determined from the ultimate shear strength $\tau_t$ according to Beltrami's expression for the uncracked material:

$$W_{2c} = \frac{\tau_t^2}{2G}. \quad (7)$$

By using the values of $\tau_t = 43$ MPa and $G$ = 1100 MPa, the critical SED for the tested PMMA is $W_{2c}$ = 0.84 MJ/m$^3$.

In parallel, the control volume definition via the control radius $R_f$ needs the knowledge of the mode I and mode II critical stress intensity factor $K_I$ and $K_{II}$ and the Poisson's ratio $\nu$, see Eqs. (3) and (4). For the considered material the resulting values are $K_{Ic}$ = 1.87 MPa m$^{0.5}$ and $K_{IIc}$ = 1.31 MPa m$^{0.5}$ (average values of data reported in [32]) which provide the control radii $R_{1c} = 0.18$ mm and $R_{2c} = 0.23$ mm, under pure tension and pure shear, respectively. In the absence of precise indications or shear tests, it is possible to approximately estimate the mode II fracture toughness $K_{IIc}$ as a function of $K_{Ic}$, according to Richard et al. [33]

$$K_{IIc} \cong \frac{\sqrt{3}}{2} K_{Ic}. \quad (8)$$

The approach proposed here is a reminiscent of the work by Gough and Pollard [34] who proposed a stress-based expression able to summarize together the results obtained from bending and tension. The criterion was extended in terms of the local SED to V-notches under fatigue loading in the presence of combined tension and torsion [35] and recently under static loading [36].

In agreement with [35, 36] and extending the method to the static case, the following expression:

**Table 4.** Experimental results. Overview of the data by using the proposed SED method for the SCB2 specimens

| $S$, mm | $W_1$, MJ/m$^3$ | $W_2$, MJ/m$^3$ | $W_1/W_{1c} + W_2/W_{2c}$ | $(W_1/W_{1c} + W_2/W_{2c})^{0.5}$ |
|---|---|---|---|---|
| 20.0 | 0.793 | 0.000 | 0.956 | 1.073 |
| 20.0 | 0.879 | 0.000 | 1.059 | 1.129 |
| 20.0 | 0.969 | 0.000 | 1.167 | 1.186 |
| 14.0 | 0.760 | 0.036 | 0.958 | 1.075 |
| 14.0 | 0.712 | 0.031 | 0.894 | 1.038 |
| 14.0 | 0.793 | 0.044 | 1.008 | 1.102 |
| 11.5 | 0.431 | 0.149 | 0.696 | 0.915 |
| 11.5 | 0.475 | 0.123 | 0.718 | 0.930 |
| 11.5 | 0.494 | 0.177 | 0.806 | 0.985 |
| 9.0 | 0.233 | 0.398 | 0.754 | 0.953 |
| 9.0 | 0.261 | 0.491 | 0.899 | 1.041 |
| 9.0 | 0.281 | 0.594 | 1.045 | 1.122 |
| 7.5 | 0.027 | 0.830 | 1.020 | 1.109 |
| 7.5 | 0.035 | 0.963 | 1.188 | 1.196 |
| 7.5 | 0.055 | 1.105 | 1.382 | 1.290 |
| 6.0 | 0.000 | 1.105 | 1.315 | 1.259 |
| 6.0 | 0.000 | 0.963 | 1.146 | 1.175 |
| 6.0 | 0.000 | 1.257 | 1.497 | 1.343 |
| 20.0 | 0.793 | 0.000 | 0.956 | 1.073 |

**Table 5.** Experimental results. Overview of the data by using the proposed SED method for the TB2 specimens

| $S$, mm | $W_1$, MJ/m$^3$ | $W_2$, MJ/m$^3$ | $W_1/W_{1c} + W_2/W_{2c}$ | $(W_1/W_{1c} + W_2/W_{2c})^{0.5}$ |
|---|---|---|---|---|
| 20.0 | 0.712 | 0.000 | 0.858 | 1.016 |
| 20.0 | 0.752 | 0.000 | 0.906 | 1.045 |
| 20.0 | 0.879 | 0.000 | 1.059 | 1.129 |
| 12.5 | 0.635 | 0.020 | 0.788 | 0.975 |
| 12.5 | 0.712 | 0.031 | 0.894 | 1.038 |
| 12.5 | 0.673 | 0.024 | 0.839 | 1.005 |
| 9.5 | 0.343 | 0.087 | 0.517 | 0.789 |
| 9.5 | 0.316 | 0.079 | 0.475 | 0.756 |
| 9.5 | 0.316 | 0.083 | 0.479 | 0.760 |
| 8.0 | 0.141 | 0.220 | 0.432 | 0.721 |
| 8.0 | 0.178 | 0.276 | 0.543 | 0.809 |
| 8.0 | 0.159 | 0.241 | 0.478 | 0.759 |
| 6.5 | 0.020 | 0.594 | 0.731 | 0.939 |
| 6.5 | 0.014 | 0.491 | 0.601 | 0.851 |
| 6.5 | 0.027 | 0.767 | 0.946 | 1.068 |
| 5.0 | 0.000 | 1.033 | 1.229 | 1.217 |
| 5.0 | 0.000 | 0.963 | 1.146 | 1.175 |
| 5.0 | 0.000 | 0.895 | 1.065 | 1.133 |

$$\frac{W_1}{W_{1c}}+\frac{W_2}{W_{2c}}=1 \tag{9}$$

is obtained. In Eq. (6) and (7) $W_{1c}$ and $W_{2c}$ are the critical values of SED under pure tension and pure shear. For the considered PMMA, $W_{1c} = 0.83$ MJ/m$^3$ and $W_{2c} = 0.84$ MJ/m$^3$. Each specimen reaches its critical energy when the sum of the weighted contributions of mode I and mode II is equal to 1, which represents the complete damage of the specimen.

The values of $W_1$ and $W_2$ have, instead, to be calculated as a function of the geometry and of the applied mode ratio

$$W_1=\frac{1}{E}\left[e_1\frac{K_I^2}{R_{1c}^{0.5}}\right], \tag{10}$$

$$W_2=\frac{1}{E}\left[e_2\frac{K_{II}^2}{R_{2c}^{0.5}}\right], \tag{11}$$

where $K_I$ and $K_{II}$ represent the mode I and mode II SIF ranges, $R_{1c}$ and $R_{2c}$ are the radii of the control volume related to mode I and mode III loadings, while $e_1$ and $e_2$ are equal to 0.1186 and 0.3332, respectively.

The detailed calculations employing the proposed criterion are reported in Tables 2–5. The square root of the left-hand side term of Eq. (9), which is, in fact, proportional to the critical load, is given in the last column of these tables.

A synthesis in terms of the square root value of the considered parameter, that is the sum of the weighted energy contributions related to mode I and mode II loading, is shown in Fig. 6 as a function of the critical load. Many of the results are inside a scatter band ranging from 0.8 to 1.2 with only few exceptions.

The fracture models proposed in this paper can be used for predicting the onset of brittle fracture in cracked PMMA components which are subjected to a combination of tension and shear loadings. The critical radii evaluated under tension and shear loadings have very close values confirming previously proposed simplified approaches [22, 23] in which the control volume size has been considered the same under tension and shear. The size of control volume is related to the size of critical or the length of the localized damage zone in PMMA which is often considered as a constants material independent of its geometry, loading condition or even mode combinations. The size of control volume determined for the PMMA material of this research was in the typical range of 0.05 to 2.00 mm reported by the researchers for PMMA [8, 11, 12, 37].

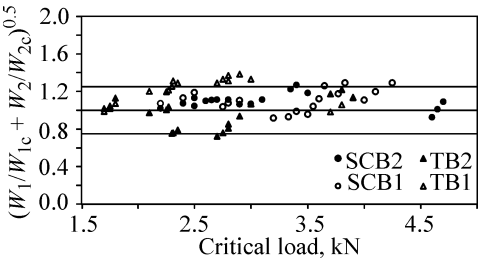


**Fig. 6.** Synthesis of the data obtained for PMMA by means of the SED approach.

## 5. CONCLUSIONS

Pure mode I, pure mode II and different intermediate mixed mode I/II fracture toughness values of commercial PMMA material were obtained experimentally using cracked specimens characterized by four different shapes. All the mixed mode PMMA fracture toughness data were predicted successfully using the SED fracture criterion. In fact, the SED approach has been found a very suitable tool to summarize all the data in a narrow scatter band. The critical radii under pure mode I and pure mode II loadings have been found very close each other confirming the engineering proposal of local mode I developed in previous contributions and used in combination with the SED approach.

## REFERENCES

1. Maccagno, T.M. and Knott, J.F., The Fracture Behaviour of PMMA in Mixed Modes I and II, *Eng. Fract. Mech.*, 1989, vol. 34, no. 1, pp. 65–86.
2. Irwin, G.R., *Fracture, Encyclopedia of Physics,* Flugge, S., Ed., Berlin: Springer Verlag, 1958, pp. 551–590.
3. Williams, M.L., Stress Singularities Resulting from Various Boundary Conditions, *J. Appl. Mech.*, 1952, vol. 19, no. 4, pp. 526–528.
4. Erdogan, F. and Sih, G.C., On the Crack Extension in Plates under Plane Loading and Transverse Shear, *J. Basic Eng.*, 1963, vol. 85, no. 4, pp. 519–525.
5. Williams, J.G. and Ewing, P.D., Fracture under Complex Stress—The Angled crack problem, *Int. J. Fract. Mech.*, 1972, vol. 8, no. 4, pp. 441–446.
6. Ewing, P.D., Swedlow, J.L., and Williams, J.G., Further Results on the Angled Crack Problem, *Int. J. Fract.*, 1976, vol. 12, no. 1, pp. 85–93.
7. Mahajan, R.V. and Ravi-Chandar, K., An Experimental Investigation of Mixed-Mode Fracture, *Int. J. Fract.*, 1989, vol. 41, no. 4, pp. 235–252.
8. Ayatollahi, M.R. and Aliha, M.R.M., Analysis of a New Specimen for Mixed Mode Fracture Tests on Brittle Materials, *Eng. Fract. Mech.*, 2009, vol. 76, no. 11, pp. 1–15.

9. Atkinson, C., Smelser, R.E., and Sanchez, J., Combined Mode Fracture via the Cracked Brazilian Disk Test, *Int. J. Fract.*, 1982, vol. 18, no. 4, pp. 279–291.
10. Awaji, H. and Kato, T., Criterion for Combined Mode I-II Brittle Fracture, *Mater. Trans. JIM*, 1999, vol. 40, no. 9, pp. 972–979.
11. Ayatollahi, M.R., Aliha, M.R.M., and Hassani, M.M., Mixed Mode Brittle Fracture in PMMA—An Experimental Study Using SCB Specimens, *Mater. Sci. Eng. A*, 2006, vol. 417, no. 1, pp. 348–356.
12. Ayatollahi, M.R., Aliha, M.R.M., and Saghafi, H., An Improved Semicircular Bend Specimen for Investigating Mixed Mode Brittle Fracture, *Eng. Fract. Mech.*, 2011, vol. 78, no. 1, pp. 110–123.
13. Saghafi, H., Zucchelli, A., and Minak, G., Evaluating Fracture Behavior of Brittle Polymeric Materials Using an IASCB Specimen, *Polym. Test.*, 2013, vol. 32, no. 1, pp. 133–140.
14. Aliha, M.R.M., Bahmani, A., and Akhondi, S., Mixed Mode Fracture Toughness Testing of PMMA with Different Three-Point Bend Type Specimens, *Eur. J. Mech. A. Solid.*, 2016, vol. 58, pp. 148–162.
15. He, M.Y., Cao, H.C., and Evans, A.G., Mixed-Mode Fracture: The Four-Point Shear Specimen, *Acta Metall. Mater.*, 1990, vol. 38, no. 5, pp. 839–846.
16. Andena, L., Corigliano, A., Frassine, R., and Mariani, S., *Mixed-Mode Crack Growth in Toughened PMMA*, Convegno IGF XVII Bologna 2004, 2008.
17. Sih, G.C., Strain-Energy-Density Factor Applied to Mixed Mode Crack Problems, *Int. J. Fract.*, 1974, vol. 10, no. 3, pp. 305–321.
18. Hussain, M.A., Pu, S.L., and Underwood, J., Strain Energy Release Rate for a Crack under Combined Mode I and Mode II, *Fracture Analysis. Proc. 1973 Nat. Symp. on Fracture Mechanics*, Part II. ASTM Int., 1974.
19. Gomez, F.J., Elices, M., Berto, F., and Lazzarin, P., Fracture of U-Notched Specimens under Mixed Mode: Experimental Results and Numerical Predictions, *Eng. Fract. Mech.*, 2009, vol. 76, no. 2, pp. 236–249.
20. Ayatollahi, M.R. and Torabi, A.R., Brittle Fracture in Rounded-Tip V-Shaped Notches, *Mater. Des.*, 2010, vol. 31, no. 1, pp. 60–67.
21. Lazzarin, P. and Zambardi, R., A Finite-Volume-Energy Based Approach to Predict the Static and Fatigue Behavior of Components with Sharp V-Shaped Notches, *Int. J. Fract.*, 2001, vol. 112, pp. 275–298.
22. Gomez, F.J., Elices, M., Berto, F., and Lazzarin, P., Local Strain Energy to Assess the Static Failure of U-Notches in Plates under Mixed Mode Loading, *Int. J. Fract.*, 2007, vol. 145, no. 1, pp. 29–45.
23. Lazzarin, P., Berto, F., Elices, M., and Gomez, J., Brittle Failures from U- and V-Notches in Mode I and Mixed I + II Mode: A Synthesis Based on the Strain Energy Density Averaged on Finite-Size Volumes, *Fatigue Fract. Eng. Mater. Struct.*, 2009, vol. 32, no. 8, pp. 671–684.
24. Berto, F. and Lazzarin, P., A Review of the Volume-Based Strain Energy Density Approach Applied to V-Notches and Welded Structures, *Theor. Appl. Fract. Mech.*, 2009, vol. 52, no. 3, pp. 183–194.
25. Lazzarin, P., Berto, F., and Ayatollahi, M.R., Brittle Failure of Inclined Key-Hole Notches in Isostatic Graphite under In-Plane Mixed Mode Loading, *Fatigue Fract. Eng. Mater. Struct.*, 2013, vol. 36, no. 9, pp. 942–955.
26. Berto, F. and Lazzarin, P., Recent Developments in Brittle and Quasi-Brittle Failure Assessment of Engineering Materials by Means of Local Approaches, *Mater. Sci. Eng. R. Rep.*, 2014, vol. 75, pp. 1–48.
27. Campagnolo, A., Berto, F., and Leguillon, D., Fracture Assessment of Sharp V-Notched Components under Mode II Loading: A Comparison among Some Recent Criteria, *Theor. Appl. Fract. Mech.*, 2016. doi 10.1016/j.tafmec.2016.02.001
28. Berto, F., Campagnolo, A., and Gallo, P., Brittle Failure of Graphite Weakened by V-Notches: A Review of Some Recent Results under Different Loading Modes, *Strength Mater.*, 2015, vol. 47, pp. 488–506.
29. Aliha, M.R.M., Bahmani, A., and Akhondi, S., Numerical Analysis of a New Mixed Mode I/III Fracture Test Specimen, *Eng. Fract. Mech.*, 2015, vol. 134, pp. 95–110.
30. Bhattacharjee, D. and Knott, J.F., Effect of Mixed Mode I and II Loading on the Fracture Surface of Polymathylmethacrylate (PMMA), *Int. J. Fract.*, 1995, vol. 72, no. 4, pp. 359–381.
31. Aliha, M.R.M., Bahmani, A., and Akhondi, S., Determination of Mode III Fracture Toughness for Different Materials Using a New Designed Test Configuration, *Mater. Des.*, 2015, vol. 86, pp. 863–871.
32. Aliha, M.R.M., Berto, F., Bahmani, A., Akhondi, Sh., and Barnoush, A., Fracture Assessment of Polymethylmethacrylate Using Sharp Notched Disc Bend Specimens under Mixed Mode I + III Loading, *Phys. Mesomech.*, 2016, vol. 19, no. 4, pp. 355–364.
33. Richard, H.A., Fulland, M., and Sander, M., Theoretical Crack Path Prediction, *Fatigue Fract. Eng. Mater. Struct.*, 2005, vol. 28, pp. 3–12.
34. Gough, H.J. and Pollard, H.V., Properties of Some Materials for Cast Crankshafts, with Special Reference to Combined Stresses, *Proc. Inst. Auto. Eng.*, 1963, vol. 31, no. 1, pp. 821–893.
35. Lazzarin, P., Sonsino, C.M., and Zambardi, R., A Notch Stress Intensity Approach to Assess the Multiaxial Fatigue Strength of Welded Tube-to-Flange Joints Subjected to Combined Loadings, *Fatigue Fract. Eng. Mater. Struct.*, 2004, vol. 27, no. 2, pp. 127–140.
36. Berto, F., Campagnolo, A., and Ayatollahi, M.R., Brittle Fracture of Rounded V-Notches in Isostatic Graphite under Static Multiaxial Loading, *Phys. Mesomech.*, 2015, vol. 18, no. 4, pp. 283–297.
37. Aliha, M.R.M. and Ayatollahi, M.R., Geometry Effects on Fracture Behaviour of Polymethylmethacrylate, *Mater. Sci. Eng. A*, 2010, vol. 527, no. 3, pp. 526–530.